An Unusual Insulator-Metal Transition in the Intermetallic Compound TiGePt

Sarah-Virginia Ackerbauer, Ewald Bischoff [1], Horst Borrmann, Ulrich Burkhardt,
Monika Gamża, Jan Gegner [2], Roman Gumeniuk, Zhiwei Hu, Andreas Leithe-Jasper,
Alim Ormeci, Reiner Ramlau, Helge Rosner, Walter Schnelle, Anatoly Senyshyn [3],
Julius C. Schuster [4], Franz Weitzer [4], Liu Hao Tjeng, and Yuri Grin

It is common knowledge that even simple elements appear in different modifications depending on external parameters like temperature and pressure. Adding the chemical composition as a new degree of freedom largely increases the flexibility of structures and the possibility for various modifications with the same stoichiometry.

In general, one expects that the corresponding phase transitions with increasing pressure or temperature lead to modifications of higher symmetry. For purely temperature-driven transitions, a reduced density for the high temperature (HT) phase is usually anticipated.

In this study we report an unusual structural phase transition of the new intermetallic ternary phase TiGePt. This compound exhibits polymorphism. The low-temperature modification (LT-TiGePt) crystallizes in the cubic MgAgAs type of structure. At 885 °C, it transforms via a reconstructive transition into an orthorhombic TiNiSi type of structure (HT-TiGePt). Thus, the transition yields a crystal structure with lower symmetry in which the atomic environment of Ti is strongly changed. This transformation is accompanied by a huge volume reduction (density increase) of over 10%. Furthermore, the associated insulator-to-metal transition reveals a complete change of the electronic structure during the structural transformation.

To shed light on the nature of this counterintuitive transition we carried out a joint experimental and theoretical study combining different diffraction techniques, thermodynamic and transport measurements, chemical analysis and electronic structure calculations.

The intermetallic compound TiGePt was synthesized from pure elemental metals in a state-of-the-art protective argon gas glove box system in an optimized metallurgical procedure. This synthesis was followed by a careful chemical, metallographical and thermoanalytical characterization. Already these basic measurements revealed that TiGePt

exists in two rather different modifications, depending in an intricate manner on temperature and small differences in the chemical composition. Although the transition is in principle reversible it is kinetically inhibited and the high-temperature phase can easily be quenched to ambient conditions. The crystal structures of the two phases were determined by a combination of powder and single crystal X-ray as well as neutron diffraction.
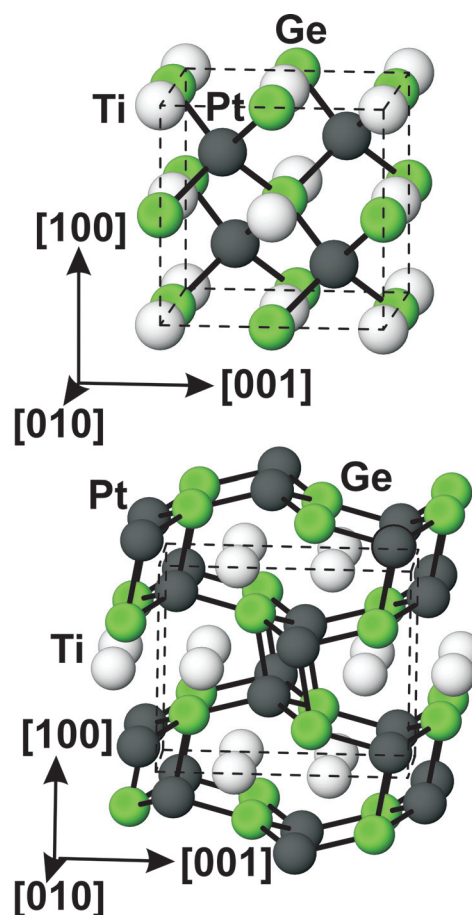

Fig. 1: Crystal structures of LT-TiGePt (cubic MgAgAs type, top) and HT-TiGePt (orthorhombic TiNiSi type, bottom). Ti, Pt, Ge atoms are shown as white, dark grey and green spheres, respectively. To facilitate the comparison between the HT and the LT structures the shortest Ge-Pt contacts are visualized.

The crystal structure of LT-TiGePt (Fig. 1, top) is of the MgAgAs type [1] (space group $F\bar{4}3m$, Pearson symbol $cF12$). In the LT phase, Ti and Ge atoms have four Pt neighbors in a tetrahedral arrangement in a distance of 2.570 Å. These rather short interatomic distances, however, contrast the open crystal structure where Pt occupies only half of the hexahedral voids in the NaCl type lattice of TiGe.

The orthorhombic HT-TiGePt modification (Fig. 1, bottom) is isotypic to TiNiSi [2] (space group $Pnma$, Pearson symbol $oP12$). This structure can be regarded as built up of layers of edge-sharing, puckered, six-membered rings of Pt and Ge atoms running perpendicular to [100]. The three Pt-Ge distances are between 2.447 Å and 2.483 Å, indicating significant interactions. The layers are inter-linked through quite short Pt-Ge contacts (2.588 Å) along the [100] direction forming a three-dimensional four-connected net. In [010] direction large eight-membered Pt-Ge rings form channels in which the Ti atoms are embedded. In consequence, this atomic arrangement results in a more dense packing of the constituents, in contrast to the expected lower density for a HT phase. Moreover, the structures of the two modifications do not show a group-subgroup relation, which is a prerequisite for a displacive transition.

The most remarkable change associated with the phase transition (LT → HT) is a huge contraction of the unit cell volume. Both unit cells contain four formula units TiGePt, hence HT-TiGePt shows about 10% higher crystal density. The dilatometry study of the LT and HT modifications directly confirms this behavior (Fig. 2): If the LT phase is heated up a strong shrinkage is observed that sets in at 896 °C (structural transition; Fig. 2, top). The observed transition is of reconstructive nature since it is characterized by a major rearrangement of atoms and the related contacts. Because there is no obvious relation between the LT and the HT structure, the question regarding the transition pathway and possible intermediate phases is difficult to answer. To investigate the latter, a sample containing the HT modification was annealed at 765 °C for just 1 h and quenched afterwards. Thus, the phase transition was stopped before its completion. This sample was conserved for the microstructural investigation.
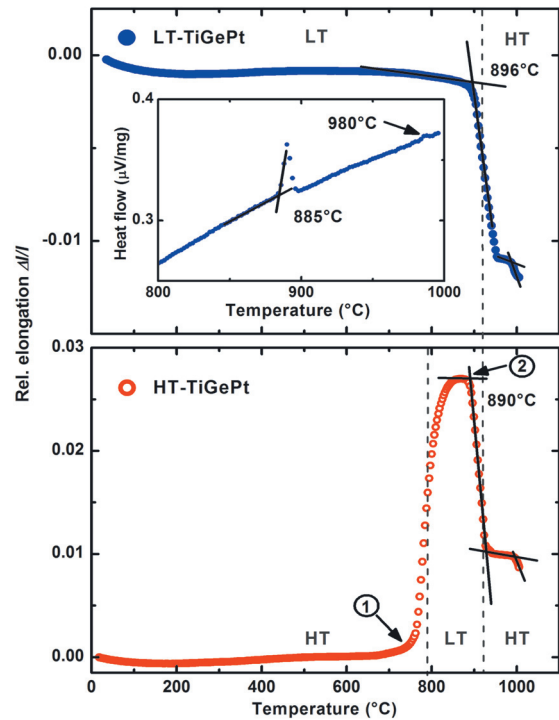

Fig. 2: Temperature dependent dilatation of LT- (upper panel) and HT-TiGePt (bottom panel). The sudden decrease in sample length at 896 °C (upper panel) is due to the LT → HT phase transition. The inset shows the DTA results with the corresponding endothermic effect at 885 °C. In the bottom panel arrow 1 indicates the temperature at which the metastable HT modification transforms under expansion into the LT modification. The temperature of the actual transition (LT phase → HT phase), which is accompanied by the 10% volume contraction, is indicated by arrow 2.

The electron backscatter diffraction maps (EBSD-maps) (Fig. 3) show the remaining large grains of the orthorhombic HT phase in different orientations surrounded by grains of LT-TiGePt, which formed at the grain boundaries. In agreement with a reconstructive transition the orientations of the grains of the LT phase are independent of the bordering grains of the HT phase (Fig. 3, middle). Moreover, no further structure, like an intermediate phase, is observed (Fig. 3, left).

To gain more insight into the electronic structure of TiGePt, the total energy, the band structure and the density of states (DOS) for both phases were calculated. In agreement with the experimental observations, the LT phase is the more stable modification. It is by 175 meV per formula unit (corresponding to about 2000 K) lower in energy than the HT phase for the experimental lattice parameters. This is well in line with the observed transition temperature of about 1160 K.
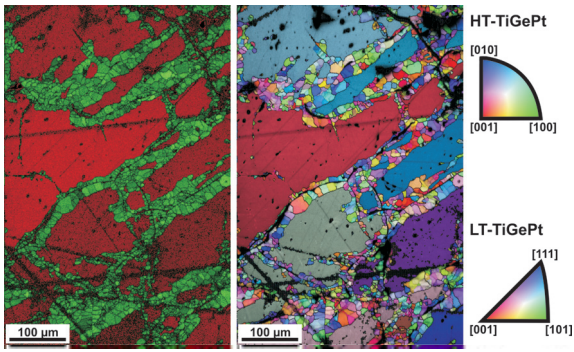
Fig. 3: EBSD maps of a TiGePt sample containing both, the LT and the HT phase, due to an incomplete transition. An overlay of a phase map and a fit map is presented (left): HT-TiGePt phase (red), LT-TiGePt phase (green). The middle panel shows an overlay of an image quality map and an inverse pole figure map. The interpretation of the grain orientations is given by a colour scheme for the inverse pole figures (legend right).
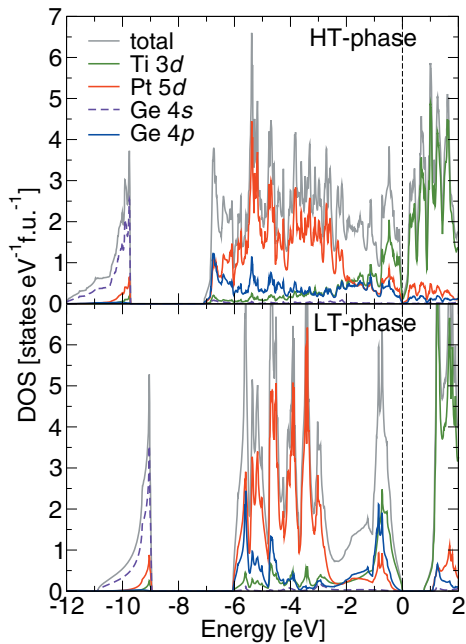

Fig. 4: Total and partial density of states (DOS) from fully relativistic electronic structure calculations of TiGePt: the results for the low-temperature (LT) phase are shown in the bottom panel and the high-temperature (HT) phase in the top panel. The common vertical dashed line indicates the position of the Fermi level.

Comparing the density of states (DOS) of the valence band of both modifications (Fig. 4), a significant difference of about 1 eV in the total band width is evident. A closer analysis shows that the shorter interatomic distances and the changed local coordination have a similarly strong influence on the change of bandwidth.
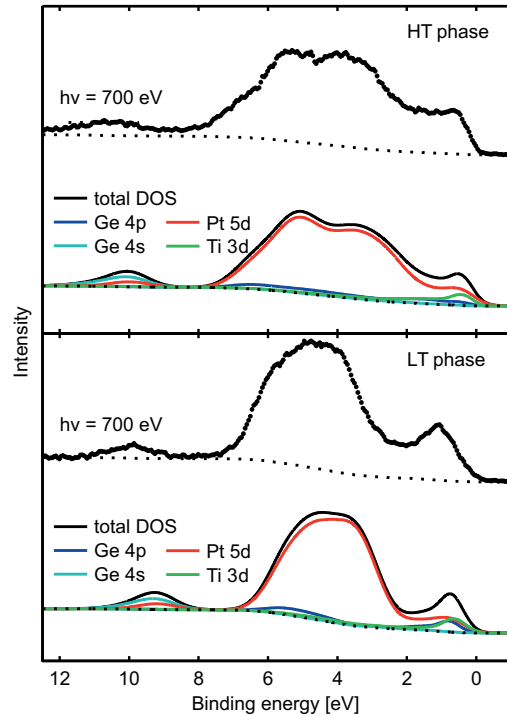

Fig. 5: Valence band spectra of the low-temperature (LT) phase (bottom panel) and the high-temperature (HT) phase of TiGePt (top panel) in comparison with the broadened and photoionization cross-section weighted partial DOS. The spectra were taken with 700 eV photon energy.

The most prominent difference between both phases, however, is the insulating character of the LT phase, in contrast to the metallic behavior of the HT modification. The LT phase exhibits a calculated gap size of about 0.9 eV, whereas the HT phase shows a pseudogap of about 0.3 eV close to the Fermi level E_F and a low value for the DOS(E_F) = 0.36 states / eV per formula unit.

To check the reliability of the calculations, we have performed photoelectron spectroscopic (PES) experiments. The spectra taken at 700 eV photon energy are shown in Figure 5. To facilitate the comparison with the band structure results, the experimental spectra of the LT phase (bottom panel) and the HT phase (top panel) are plotted together with their respective calculated DOS. The partial DOS are multiplied with the Fermi-Dirac distribution function, weighted by their respective tabulated photoionisation cross-sections, and broadened to account for the experimental resolution and lifetime effects. Finally, the commonly used integral-type of background – as indicated by the dotted lines – is added to account for the presence of secondary electrons during the photoemission process.

An extremely good correspondence between the computational and the experimental results can clearly be seen in Figure 5. The essential features in the experimental data are all well reproduced, including the energy gap between the Ge 4s-like shallow core states and the remainder of the valence band. The experiment confirms that most of the Pt 5d spectral weight is concentrated at the high-binding-energy side of the valence band, and that the Ti 3d states contribute significantly to the features near the Fermi level. Most importantly, the broadening of the Pt 5*d* and Ti 3*d* derived bands in the HT phase as compared to the LT phase is also clearly revealed by the experiment.

The theoretical results regarding the metallicity of the two phases are confirmed by resistivity measurements. For the LT modification the resistivity ρ increases with decreasing temperature between 400 K and 200 K, indicating semiconducting behavior (Fig. 6, top). The origin of the almost constant resistivity below 200 K and the additional low-temperature upturn cannot be identified unambiguously at present, but is likely due to the presence of impurity-related states in the gap. In contrast, the HT phase shows, down to about 50 K, an essentially linear decrease of ρ, as expected for metallic behavior (Fig. 6, bottom). The absolute values for the resistivity of HT-TiGePt are typical for bad metals and almost four orders of magnitude smaller than for the semiconducting LT phase. The upturn of ρ below 50 K in HT-TiGePt remains at present unclear. According to the susceptibility data $\chi(T)$, it can neither be explained by a magnetic origin nor by extrinsic paramagnetic impurities. Consistent with the low calculated DOS at E_F, a rather small $\chi(T)$ is observed, which is nearly temperature independent apart from a small Curie tail at low temperatures. The susceptibility of the LT phase is very small and featureless, indicating non-magnetic behavior.

The chemical bonding in the LT and the HT modifications of TiGePt was investigated by a combined topological analysis of the electron localizability indicator (ELI) and electron density (ED), calculated both by the FPLO and the TB-LMTO-ASA schemes.

The ELI distribution computed by FPLO (Fig. 7) reveals the penultimate shell (5th shell) of Pt being clearly structured in LT-TiGePt (Fig. 7, top left), while in the high-temperature case a weaker structuring can be seen (Fig. 7, top right). The topology of the structuring (positions of the reduced values
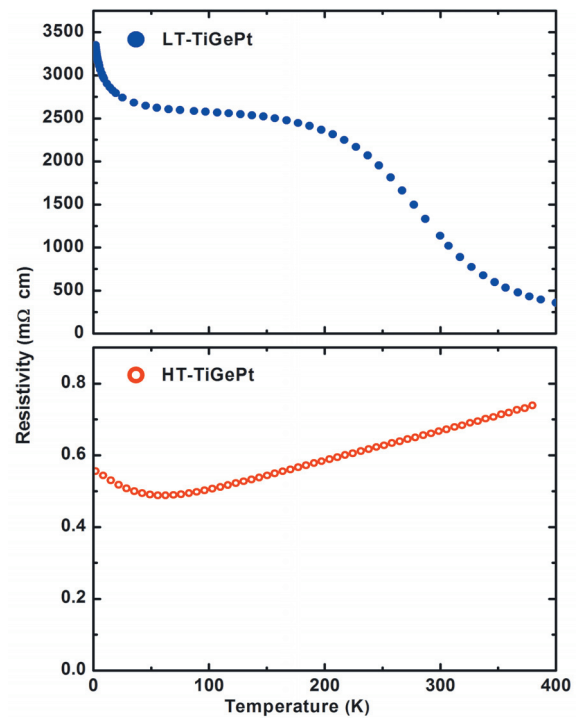

Fig. 6: Temperature dependence of the electrical resistivity measured on polycrystalline samples of LT- (top) and HT-TiGePt (bottom).

in the shell) in LT-TiGePt implies contributions of penultimate-shell electrons (most probably 5*d*) mainly to the Ti-Pt interactions, and only partially to the Ge-Pt interactions.

Furthermore, the Ti penultimate shell is also structured in both modifications. In the LT form, the particular way this structuring takes place (lower-ELI-value regions facing Ge positions, Fig. 7 middle left) implies that the Ti penultimate (3rd) shell electrons (most probably 3*d*) contribute to interactions with the Ge atoms. However, the analysis of the bonding interactions in the valence region in LT-TiGePt (Fig. 7, bottom left) reveals two attractors in front of the 'hole' in the inner shell of Ti. Each attractor should visualize a three-center bond Ge-Pt-Ti bond. In practice, it mainly reflects the ring attractor of the Ge-Pt bond.

Resulting from its atomic arrangement, Ti seems to make some, but not the decisive, contribution to this interaction. Thus, the corresponding attractors are considered as fingerprints of Ge-Pt interactions. The next striking interaction in the LT-TiGePt is a two-center bond Ti-Pt bond, whose attractor is located on the line between the atoms.
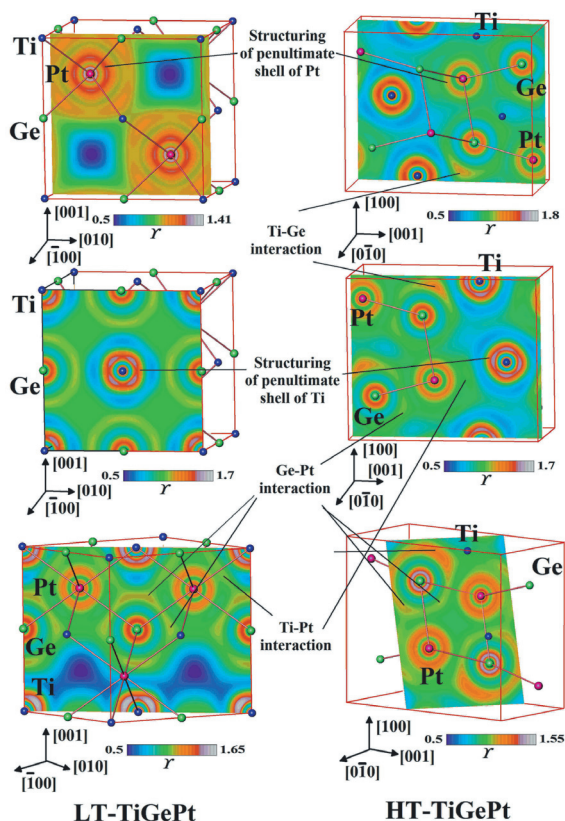
Fig. 7: Electron localizability indicator in LT- and HT-TiGePt.

The HT modification exhibits six different types of attractors. Two of them visualize multi-centre bonds whereas four of them show two-center bonds. The former are six-centre bonds involving one Ge, three Pt (nearest neighbours of Ge), and two Ti (two of the five near neighbours of Ge). Taking into account the contributions of each atom these interactions are identified as mainly Ti-Ge interaction (Fig. 7, top and middle right), and as mainly Ge-Pt interaction (Fig. 7, middle and bottom right). The latter group of bonds is formed by Ti and Pt atoms. The corresponding attractors are difficult to identify (Fig. 7, middle right). Integration of the electron density in basins of the Ti-Pt-bonding attractors gives 3.5 and 1.8 electrons per formula unit for the LT and the HT modification, respectively. This reveals a remarkable reduction

of the Ti-Pt bonding basin's population during the LT-to-HT transition. The electron count in the basin of a three-centre Ge-Pt-Ti bond is about half an electron yielding a total of 6.4 electrons per formula unit. On the other hand, in the HT modification each six-centre bond basin contains 3.0 and 2.1 electrons (7.2 electrons per formula unit), indicating a significant increase in the number of multi-centre bonding electrons on the basis of individual basins.

In total, the Ge-Pt interaction is present in both modifications of TiGePt, albeit as a part of multi-centre bonding. The Ti-Pt interaction in the LT modification is strong, but significantly reduced in the HT modification. The Ti-Ge interaction is not very pronounced in the LT modification, yet becomes essential in the HT modification, albeit again as a main part of multi-centre bonding.

In conclusion, we found an unusual volume contraction (density increase) associated with the phase transition of LT-TiGePt to HT-TiGePt. An accompanied insulator-to-metal transition was observed. The structural changes are related to significant changes of the atomic interactions, yielding a pronounced difference of the resulting electronic structures. This difference is well reflected in the experimental results.

References

[1] *H. Nowotny and W. Sibert,* Z. Metallkd. **33** (1941) 391.
[2] *C. Shoemaker and D. Shoemaker,* Acta Crystallogr. **18** (1965) 900.

[1] Max-Planck-Institut für Intelligente Systeme, Heisenbergstraße 3, 70569 Stuttgart, Germany
[2] II. Physikalisches Institut, Universität zu Köln, Zülpicher Straße 77, 50937 Köln, Germany
[3] Forschungsneutronenquelle Heinz Maier-Leibnitz FRM-II, Technische Universität München, Lichtenbergstraße 1, 85747 Garching bei München, Germany
[4] Innovative Materials Group, Universität Wien, Währinger Straße 42, 1090 Wien, Austria